ICANS-XIV
The 14th Meeting of the International Collaboration on Advanced Neutron Sources
June 14-19, 1998
Starved Rock Lodge, Utica, Illinois

Proton Energy Dependence of Reflector Effect on a Beam Intensity from a Decoupled Water Moderator

R. Takagi and Y. Kiyanagi
Graduate School of Engineering, Hokkaido University, Sapporo 060-8628, Japan

Abstract

We studied change of relative beam intensities from a decoupled H_2O moderator with various reflector materials as a function of proton energy. We estimated the effect of secondary neutrons produced by spallation and (n,2n) reactions in the reflector, and found that the effect of the reflector changes depending on the proton energy. For proton energies below about 0.5 GeV beryllium was the best and above this energy lead was the best among the material studied.

1. Introduction

So for, beryllium have been used as a reflector in the existing pulsed spallation sources. However, the neutronic studies on reflector have been done[1]~[8], but proton energy dependence have not been studied. The result obtained by electron linac experiments indicated that Be (or BeO) was the best among graphite, lead and beryllium although the target-moderator-reflector assembly (TMRA) was very simple[9]. However, it was suggested that the effect of the reflector would depend on the spatial distribution of fast neutrons emitted from a target. Furthermore, in the case of the spallation neutron source the reflector works as a part of the target; namely, the reflector is another fast neutron source and the spatial distribution of the fast neutrons becomes wider with proton energy. On the other hand the fast neutrons produced by an electron linac is usually point like and there are no extra spallation neutrons. So, some difference will be expected between the electron source and the spallation source.

Recently, it is said that lead shows good neutronic performance from calculational results for spallation neutron sources. These results suggest that the proton energy dependence of the reflector effect is different between moderating and non-moderating reflectors.

Therefore, we intended to study the reflector effect as a function of the proton energy so as to understand the reflector effect systematically. We measured intensities and pulse

Keywords: Reflector, Energy dependence, Secondary neutron

shapes by using an electron linac and also calculated neutron intensities from moderators with several kinds of reflector materials at various proton energies by the LAHET Code System (LCS).

2. Experiments by using an electron linac

First, we measured the neutron intensities and the pulse shapes from a moderator with graphite or iron reflectors. We chose graphite as one of the moderating materials since beryllium is so expensive and chose iron since it has relatively large absorption cross section. Therefore, we expected that even in a coupled system the pulse may not be widened so much in the iron case. We also use the experimental results as a benchmark test of the calculations.

The experimental geometry is shown in Fig.1. We used the Hokkaido linac as a neutron generator. The target material was lead with a dimension of 7x7x7 cm^3. The size of H_2O moderator was 4.5x10x10 cm^3. The experiments were performed for the coupled and the decoupled H_2O moderators. For decoupler material we used B_4C (decoupling energy 2.5eV). Figure 2 shows energy spectra from the moderator. The shapes of the spectra are almost the same. The intensity from the decoupled moderator with the iron reflector is lowest but the intensity from the coupled moderator is higher than that from a decoupled moderator with graphite reflector. The intensity from a coupled moderator with graphite is much higher than the others. The relative intensities are summarized in Table 1.

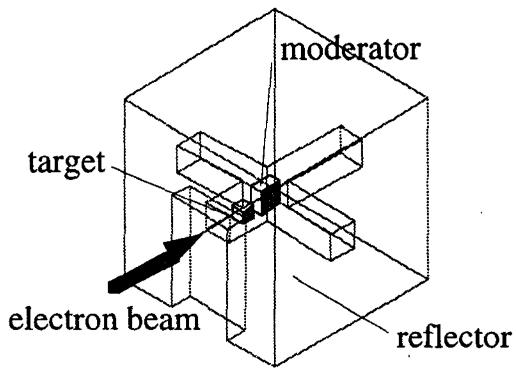

Fig.1 Experimental geometry

We also measured the pulse shapes from a moderator with the graphite and the iron reflectors in the case of the decoupled and the coupled systems. An example of the pulse shapes is shown in Fig.3. The pulse width of the coupled moderator with the iron reflector is not so broadened. Fig.4 shows pulse widths in full width at half maximum (FWHM). The FWHM's are slightly larger in the case of the coupled iron reflector than the decoupled graphite reflector. The difference is only about 20% in the thermal neutron region. The values of the iron coupled case approaches to the decoupled ones at higher energy. The FWHM's of the coupled graphite reflector are smaller than we expected but the pulse shape has long tail due to the slowing down in the graphite reflector as shown in Fig. 5. To estimate the effect of this tail we calculated the mean emission time by using the experimental results. They are summarized in Table 2. The values of the coupled graphite case are one order of magnitude larger than those of the coupled iron reflector. These results suggest that a coupled iron reflector will be used in the spallation source. Therefore, we decided to include a coupled iron reflector in the following studies by simulation.

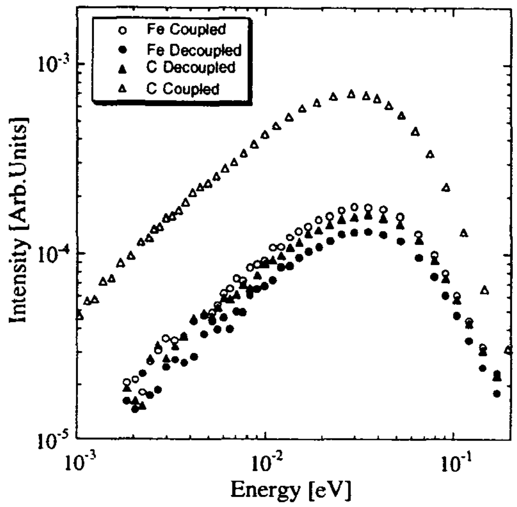

Fig.2 Energy spectra from a water moderator

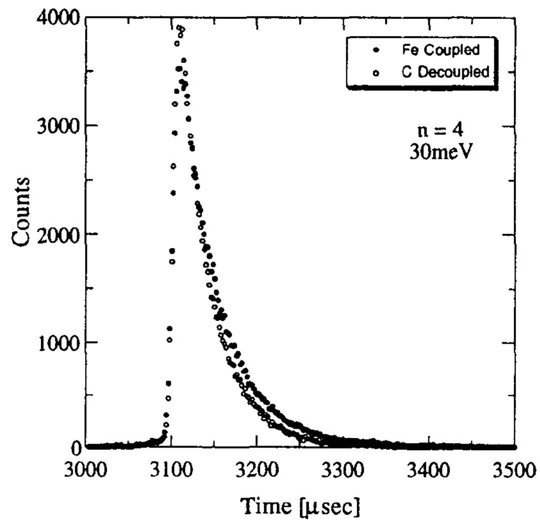

Fig.3 Pulse shapes in the case of coupled iron reflector and decoupled graphite reflector

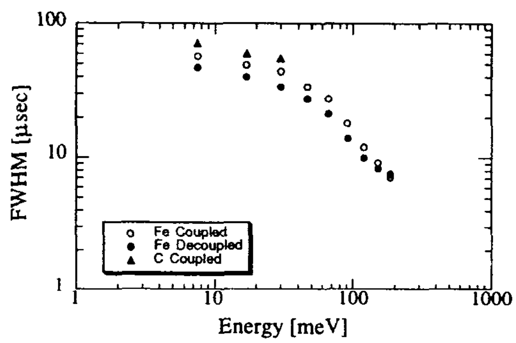

Fig.4 Pulse width in FWHM for a moderator with graphite and iron reflector

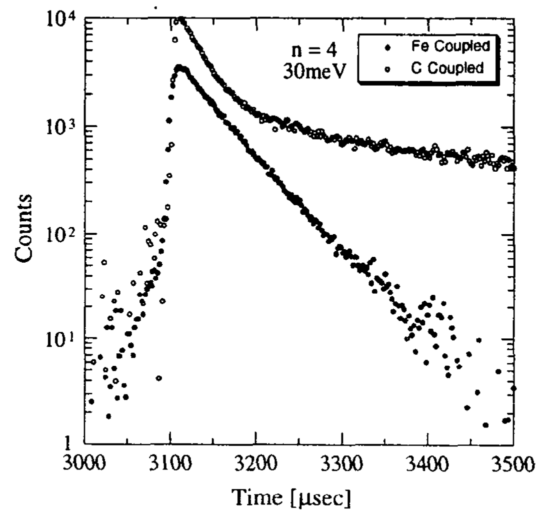

Fig.5 Pulse shapes from a coupled moderator with graphite and iron reflector

Table 1 Intensity ratios obtained by experiments and calculations

reflector type	experiment	calculation
Fe Coupled	1.000	1.000
Fe Decoupled	0.753	0.747
C Coupled	3.317	2.953
C Decoupled	0.921	0.935

Table 2 Mean emission time in the case of graphite and iron reflector

Energy [meV]	Fe Coupled	C Coupled
7.5	66.2	688
17	57.3	644
30	56.4	510

Then, calculations were performed on the same geometries by using LAHET Code System (LCS). For cross section data, ENDF/B-V was used. Relative intensities obtained by calculations are also shown in Table 1, these results were normalized by the intensity of the coupled H_2O moderator with iron reflector. It is found that the intensity ratios obtained by calculations agree very well with those by experiments. Therefore, it is said that LCS can simulate the experiment accurately.

Then, we performed the calculations in order to analyze the proton energy dependence of the neutron intensity from moderators with various reflector materials.

3. Proton energy dependence of neutron intensity from moderators

3-1. Calculations

In the spallation neutron sources, neutrons are not only produced in a target but also in a reflector. Therefore, we must also take into account the effect of reflector as neutron source when we consider TMRA. Main processes of neutron production in the reflector are spallation reaction and (n,2n) reaction. So, we estimated the effect of the neutrons produced in the reflector by spallation reaction and (n,2n) reaction by simulation using the LCS.

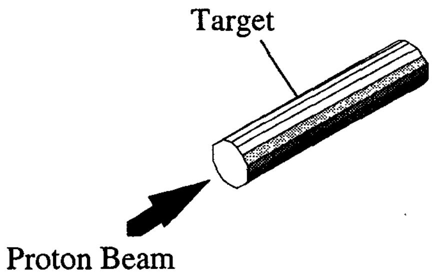

Fig.6(a) Geometry used for calculation (target)

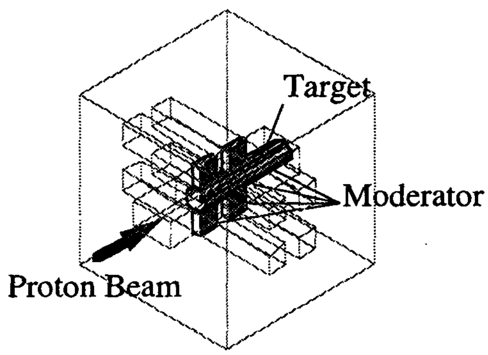

Fig 6(b) Geometry used for calculation (TMRA)

Geometries used in the calculations are shown in Fig.6(a) and Fig.6(b). Fig.6(a) is a geometry of a cylindrical target only. Target is a homogeneous mixture of tungsten and 10% D_2O coolant with the dimension of 10 cm (diam.) x 57.2 cm (length) at 3 GeV proton beam. The target length was adjusted depending on the proton energy. The profile of the proton beam is parabolic with a size of 3.5 cm in diameter on the incident surface of the target. Proton energies 0.12, 0.2, 0.5, 0.8, 1, 2 and 3 (GeV) are studied. Fig.6(b) is a geometry of TMRA. Target is surrounded by D_2O coolant. Four water moderators are located above and below the target. These are decoupled H_2O with the dimension of 5x10x10 cm^3. For decoupler material we chose B_4C (decoupling energy 2.5 eV). The distance between the target surface and moderator surface is 2 cm. As reflector materials, beryllium, graphite, iron and lead are studied.

LCS consists of two main codes, LAHET and HMCNP. The LAHET simulates the transport and interaction of high energy particles above cut off energy, and the HMCNP simulates them in the energy region below cut off[10]. We used a cut off energy of 15MeV.

We performed full system calculations by using the LCS. We also performed 2 step calculations to estimate contributions of neutrons produced by (n,2n) in the reflector. First we calculated sub 15MeV neutron production only in target by using the LAHET and second the sub 15MeV neutrons were transported to the full system of TMRA by using data obtained by the LAHET calculation. These calculations were done by the HMCNP code. From this calculation, we can estimate the number of neutrons produced by (n,2n) reaction in the reflector caused by sub 15 MeV neutrons. By comparing the results of these two type calculations we can obtain the neutrons produced in the process of high energy particle transportation, which are considered to be mainly due to the spallation.

3-2. Neutron numbers produced in TMRA

First we calculated the neutron yields in the TMRA. The results are shown in Table 3. The ratios of neutron yields of each process to that only in the target are also written in % in the parentheses. It is found that with increasing proton energy, contribution of the neutrons produced by the spallation reaction in the reflector increases especially in lead and the ratio of neutrons produced by (n,2n) reaction in reflector does not depend so much on the proton energies. The contribution of (n,2n) reaction is remarkable in beryllium.

Table 3 The number of neutrons produced in reflectors [n/p]
( ): ratio (%) to the yield in the target

Proton Energy	W Target	Be reflector		C reflector		Fe reflector		Pb reflector	
[GeV]	[n/p]	spallation	(n,2n)	spallation	(n,2n)	spallation	(n,2n)	spallation	(n,2n)
0.12	0.42	0.05 (10.9)	0.07 (16.3)	0.02 (5.4)	0.00 (0.0)	0.06 (14.1)	0.00 (1.0)	0.09 (22.3)	0.01 (3.5)
0.2	1.18	0.16 (13.4)	0.18 (15.4)	0.08 (6.4)	0.00 (0.0)	0.24 (20.1)	0.01 (1.0)	0.39 (32.9)	0.04 (3.4)
0.5	6.61	0.92 (14.0)	0.86 (13.1)	0.46 (7.0)	0.00 (0.0)	1.72 (26.1)	0.05 (0.8)	2.87 (43.5)	0.18 (2.7)
0.8	13.9	1.95 (14.1)	1.84 (13.3)	1.05 (7.6)	0.00 (0.0)	3.82 (27.5)	0.10 (0.7)	6.19 (44.6)	0.38 (2.7)
1	18.2	2.53 (14.0)	2.62 (14.5)	1.25 (6.9)	0.00 (0.0)	5.16 (28.5)	0.14 (0.8)	8.58 (47.3)	0.55 (3.0)
2	36.6	5.52 (15.1)	6.33 (17.3)	2.78 (7.6)	0.00 (0.0)	11.59 (31.7)	0.37 (1.0)	19.7 (53.8)	1.42 (3.9)
3	53.1	8.80 (16.6)	9.79 (18.5)	4.59 (8.7)	0.00 (0.0)	17.52 (33.0)	0.63 (1.2)	29.2 (54.9)	2.31 (4.4)

3-3. Comparison of Neutron intensities from moderators

In older to study the proton energy dependence of the efficiencies of various reflector materials, we compare the intensities from the moderators. Here we normalized the intensity by the one in the case of the decoupled lead reflector. Figure 7 shows relative neutron intensities from moderators in the case where contributions from the secondary neutrons are excluded. This indicates the pure efficiency as a neutron reflector. Figure

7(a) is the intensities only from upstream two moderators. The relative intensities in the cases of beryllium and graphite increase with decreasing the proton energy. These two are the moderating reflector. Therefore, they are efficient when neutrons are produced near the moderators due to the short slowing-down length. Figure 7(b) shows the relative total intensities from all four moderators. In this case graphite is better than beryllium since probably it has longer slowing-down length than beryllium. The results suggest that the spatial distribution of the fast neutrons from a target surface is important. Figure 8 shows the spatial distributions from target surface, which clearly shows broadening with the proton energy. We estimated the width of the distributions by the standard deviations and Fig.7(a) and Fig.7(b) were replotted as a function of the standard deviation. The result is shown in Fig.9(a) and 9(b). From these figures, it is found that the efficiency of beryllium and graphite become worse in the region of standard deviation greater than 4 cm.

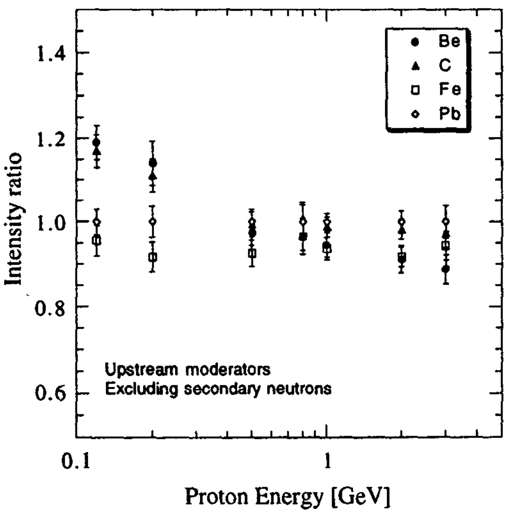

Fig.7(a) Relative neutron intensities from upstream moderators excluding secondary neutrons

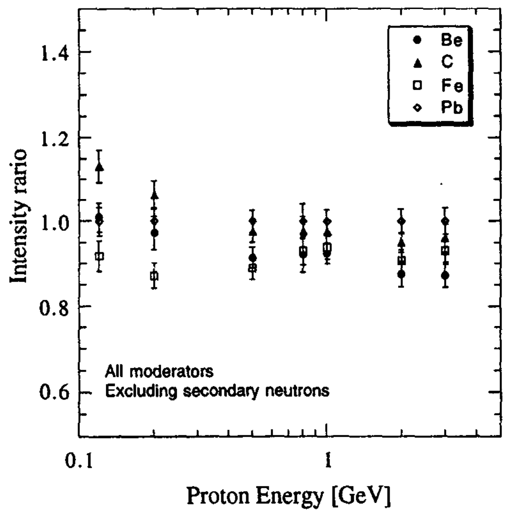

Fig.7(b) Relative neutron intensities from all moderators excluding secondary neutrons

Next, we studied effect of (n,2n) reaction. The results for upstream moderators and that for all moderators at various proton energies are shown in Fig.10(a) and Fig.10(b). When we compare Fig.10(a) with Fig.7(a), it is found that the neutron intensity in the case of beryllium reflector becomes relatively much higher over whole proton energies. The superiority of the beryllium reflector is weakened again when compared the total intensities as shown in Fig.10(b). It is due to the fact that the number of neutrons produced by (n,2n) reaction in reflector is much larger in beryllium than the others, as expected from the results indicated in Table 3.

The results obtained by the full system calculations including all produced neutrons are shown in Fig.11(a) for the upstream moderators and Fig.11(b) for all moderators,

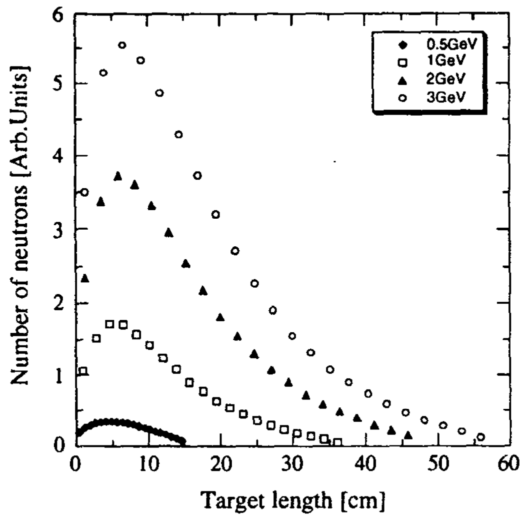

Fig.8 Neutron spatial distributions from a target surface

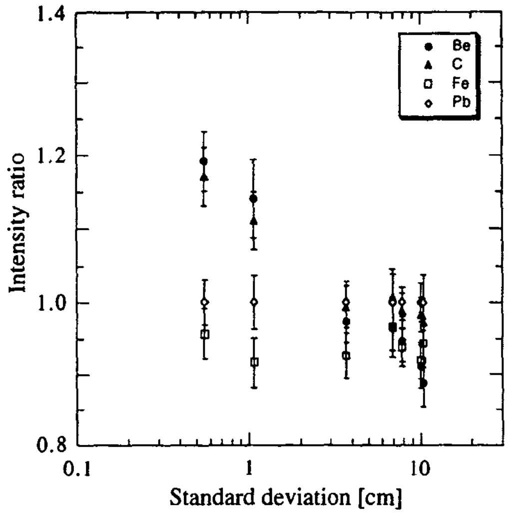

Fig.9(a) Relative neutron intensities from upstream moderators as a function of standard deviations in the case excluding secondary neutrons

respectively. The intensities in the lead reflector case increase compared with the intensities in other cases discussed before due to the contribution of the neutrons produced in the reflector especially in the higher proton energies since the contribution of the neutrons produced by spallation increases with the proton energy.

We also calculated the intensities in the case of the coupled lead and the iron reflectors as references. The intensity in the case of the coupled iron is much higher than that in the decoupled lead case. If it is still true that the pulse width is not broadened in a coupled iron case in the spallation source, iron will be one of the candidates. The intensity in the case of the coupled lead reflector is higher than that in the coupled iron. Lead moderate neutrons very slowly. Therefore, broadening of pulse width of neutrons from a moderator may not so large. To confirm this, it is necessary to measure the pulse shapes of these coupling systems. The intensity from the upstream moderators in the case of the lead reflector crosses with that in beryllium case around 0.5

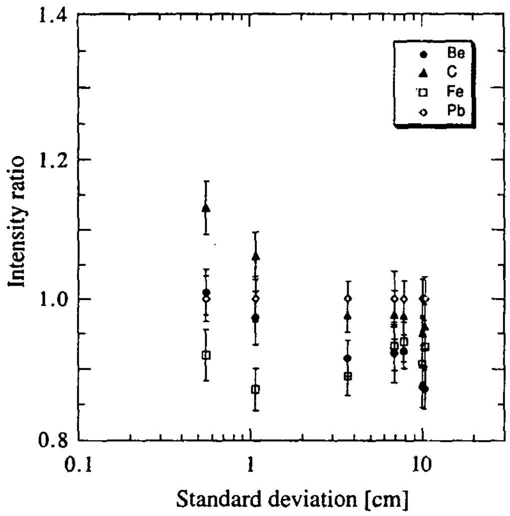

Fig.9(b) Relative neutron intensities from all moderators as a function of standard deviations in the case excluding secondary neutrons

GeV. this indicate the upper limit of the proton energy where the beryllium reflector is superior to the lead reflector.

Finally, we summarize the contributions of the secondary neutrons at 3 GeV protons in Fig.12. The efficiency as a reflector seems to be independent of atomic number above carbon. As expected the merits of beryllium at this proton energy is (n,2n) reaction and that of lead is spallation. The difference in intensities are mainly caused by the neutron production by these two reactions.

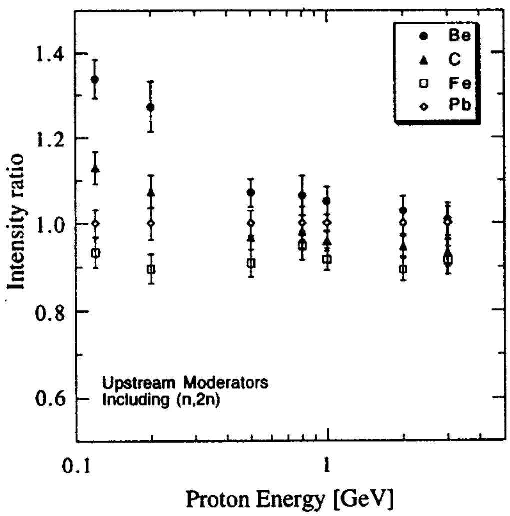

Fig.10(a) Relative neutron intensities from upstream moderators in the case including (n,2n) reaction

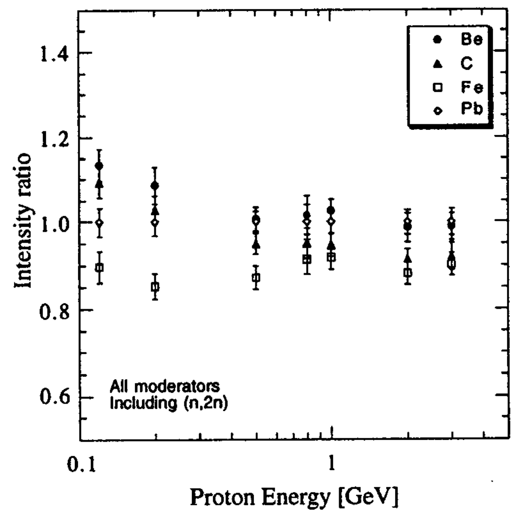

Fig.10(b) Relative neutron intensities from all moderators in the case including (n,2n) reaction

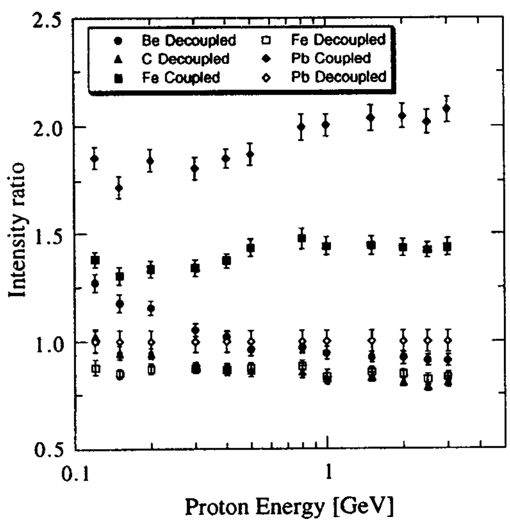

Fig.11(a) Relative neutron intensities from upstream moderators in the case including all neutrons produced

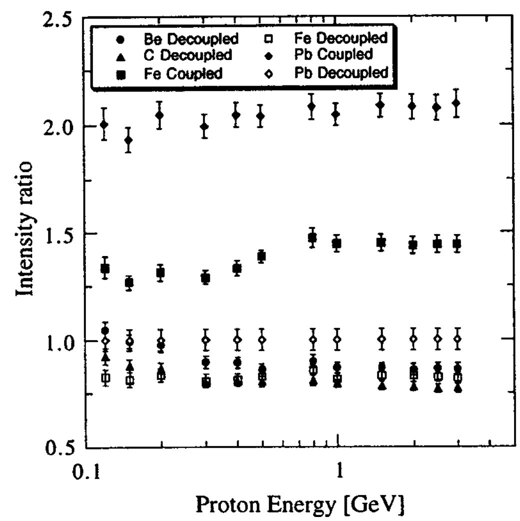

Fig.11(b) Relative neutron intensities from all moderators in the case including all neutrons produced

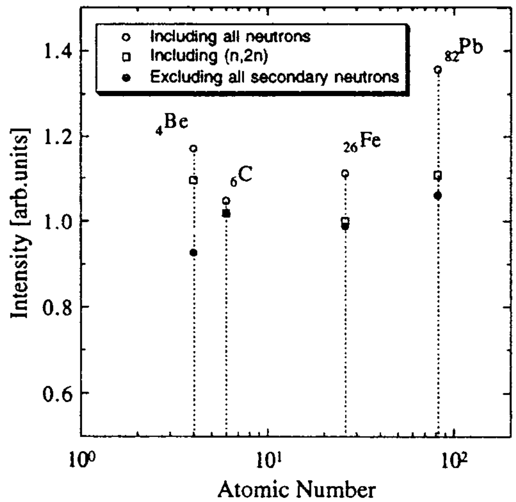

Fig.12 The effects of secondary neutrons on neutron intensities from moderators at 3 GeV

4. Conclusion

The contribution of the neutrons produced in a TMRA by spallation reaction increase with the proton energy and also with atomic number. It has become clear that a moderating type reflector is effective at lower proton energy since the spatial distribution of the emitted fast neutrons at a target surface is narrow. Beryllium is effective in the proton energy below about 0.5 GeV. Lead is the best among the materials studied here above this energy due to the contribution of the neutrons produced by spallation. A coupled reflector of iron should be studied in more detail since it may be able to remove the decoupler, cooling of which is not so easy.

5. References

[1] J.M. Carpenter: G.J. Marmer, ANL-sss-72-1 (1972).

[2] B.C. Boland et al.: RL-77-140/A (1977).

[3] A.D. Taylor: RL-81-057 (1981).

[4] K. Inoue et al.: J. At. Energy Soc. Jpn., (in Japanese), 21[11], 865 (1979).

[5] K. Inoue et al.: Nucl. Instrum. Methods, 192, 129 (1982).

[6] G.S. Bauer et al.: Proc. ICANS-V, p. 475 (1981).

[7] A.D. Taylor: ibid., p. 377.

[8] G.J. Russel et al.: ibid., p. 389.

[9] Y. Kiyanagi: J. Nucl. Sci. Tech., 24, 490 (1987).

[10] R.E. Prael and H. Lichtenstein, "User guide to LCS: The LAHET code system", LA-UR-89-3014 (1989).